Cavitation erosion of the calcium carbonate deposits

Boštjan Pečnik*

Jožef Stefan International Postgraduate School,
Jamova cesta 39,
1000 Ljubljana, Slovenia and Gorenje d.d.,
Partizanska 12, 3503 Velenje, Slovenia
Email: bostjan.pecnik@gorenje.com
*Corresponding author

Roman Šturm, Marko Hočevar, Matevž Dular and Brane Širok

Faculty of Mechanical Engineering,
University of Ljubljana,
Aškerčeva 6, 1000 Ljubljana, Slovenia
Email: roman.sturm@fs.uni-lj.si
Email: marko.hocevar@fs.uni-lj.si
Email: matevz.dular@fs.uni-lj.si
Email: brane.sirok@fs.uni-lj.si

Abstract: The paper presents the research of erosion effects caused by acoustic cavitation on metallic and enamelled specimens coated with calcium carbonate – scale. The deposition of calcium carbonate was performed under controlled laboratory conditions. The deposition took place at the same integral conditions to the specimens of different surface roughness. Cavitation as a cause of erosion was generated in a vessel with ultrasonic excitation. Simultaneously with the monitoring of cavitation above the specimens, the destruction of scale on the surface of specimens was analysed. The results of experiments indicate a characteristic effect of cavitation intensity on the destruction of scale surface layer. The intensity of cavitation erosion is proportional to the voltage on the sonotrode or the intensity of pressure fluctuations, and depends on the roughness of the surface of specimens, on which the scales were deposited.

Keywords: cavitation erosion model; scale; cavitation; material properties.

Reference to this paper should be made as follows: Pečnik, B., Šturm, R., Hočevar, M., Dular, M. and Širok, B. (2015) 'Cavitation erosion of the calcium carbonate deposits', *Int. J. Microstructure and Materials Properties*, Vol. 10, Nos. 5/6, pp.445–462.

Biographical notes: Boštjan Pečnik received his Bachelor of Science degree at the University of Ljubljana, Faculty of Mechanical Engineering in 1995. He has close to 20 years experiences in household appliances business in the field of R&D, product management and production. He was Head of Cooking Appliances R&D in Gorenje Group from 1997 to 2002. From 2002 to 2003, he was Head of R&D for small motorised appliances in Bosch und Siemens Haushaltsgeräte Department in Nazarje, Slovenia. Since 2006, he is an Executive Director for R&D of the Gorenje Group.

Roman Šturm is an Associate Professor at the Faculty of Mechanical Engineering, University of Ljubljana, Slovenia. His main field of interest is laser surface heat treatment, and materials characterisation. Till now, he had published more than 40 scientific articles and had presentations at more than 60 international conferences. In the past he worked in industry. After that he was four years the Head of Laboratory for Creep Testing at the Institute of Metals and Technology, Slovenia. Now, he is the Head of Laboratory for heat treatment, and vice dean of the Faculty of Mechanical Engineering.

Marko Hočevar has received a BSc in Physics in 1996. Later, he worked in Turboinstitut, Institute for Turbine Machinery until 2000. Later, he worked at the Faculty of Mechanical Engineering, University of Ljubljana as Assistant and 2011 as an Associate Professor. He is involved in experimental work in a broad field of energy engineering. Until now, he has published more than scientific journal 60 papers with review.

Matevž Dular finished his undergraduate studies in 2002 at the University of Ljubljana. He then worked as a PhD student at the TU Darmstadt. Later, he was for two years and was a project manager of high temperature pump development at the Hidria Corporation. He was appointed as an Assistant Professor in 2007 and as an Associate Professor in 2012. His main fields of interest include general fluid mechanics, turbine machinery, cavitation, erosion, computational fluid dynamics and visualisation. He authored 42 reviewed journal papers. He advised six PhD and 20 BSc or MSc students.

Brane Širok has received a BSc from Faculty of Mechanical Engineering, University of Ljubljana in 1980. Later, he was Head of Applied Aerodynamics Department at Turboinstitut, Institute of Turbine Machinery. In 1996, he moved to a position of Professor Faculty of Mechanical Engineering, where he is a dean since 2013. His research interests are flow and process visualisation, experiment-based modelling and turbine machinery. He authored more than 150 reviewed journal papers.

1 Introduction

The accumulation of $CaCO_3$ (scale) is one of significant disturbances that affects a series of industrial processes, such as the membrane filtration (desalination) and heat transfer. The heat exchangers include two effects: the first one, where the heat transfer from the water to the heat exchanger wall is reduced already in case of thin scale layers, and the second one, where the scale acts as a thermal insulator causing the overheating of heating bodies that result in their malfunctions. The scale deposits may also cause a characteristic decrease of pipe flow. In the households in a hard water environment, the function and energy efficiency of machines is decreased in case of household appliances, such as boilers and washing machines. This causes additional operational costs as a result of servicing, parts replacement and higher electricity bills up to 25% (DOE, 2011). Currently, the use of chemicals is the most efficient method for preventing scale deposits. However, chemicals are expensive and prone to environmental concerns. We therefore search for cheaper and environment-friendly procedures, where, as stated in recent review (Hasson et al., 2011), the most promising green scale inhibitors are based on polyaspartic acid. Among them are the methods with surface treatment lime layer

(MacAdam and Parsons, 2004). The purpose of this paper is to present ultrasonic cavitation as a promising hydrodynamic procedure for the scale removal. The paper will present an evaluation of the impact of ultrasonic cavitation on the removal of calcium carbonate deposited on a metallic and enamelled surface with different roughness. It will include the research of the parameters of roughness and intensity of ultrasonic cavitation on the removal of calcium carbonate, which will be assessed using a visualisation comparison method on a macro-scale.

The formation of $CaCO_3$ (scale) is a complex process that depends on numerous factors, such as the level of oversaturation, the composition of fluid, the temperature, the hydrodynamic – flow conditions and the properties of surfaces on which it accumulates, such as the surface energy and roughness (MacAdam and Parsons, 2004; Karabelas, 2002). The dissolved CO_2 in water forms a weak carbon acid that dissociates into hydrogen carbonate, hydrogen and carbonate ions. Calcium ions react with bicarbonate which then exists in balance with calcium carbonate and carbon dioxide. The entire reaction may be written as

$$Ca^{2+} + 2HCO_3^- \rightarrow CaCO_{3(s)} + CO_{2(g)} + H_2O$$

The physical process of the formation of solid structure of $CaCO_{3(s)}$ includes the formation of ions, clustering, nucleation and growth of crystals in agglomerated clusters on solid surfaces. Calcium carbonate is formed in different polymorphic crystal forms, which, in spite of the fact that they are chemically identical, have different crystal structures, which is why they differ in the macro- and micro-structural properties. Calcium carbonate may appear in the form of three crystal structures: vaterite, aragonite and calcite (Elfil and Roques, 2001). Calcite and aragonite are the most common polymorphic structures.

Factors that affect the level of deposition, the extent and type of polymorphic structure on solid walls, include the following: pH factor, temperature T, flow conditions in a liquid at solid walls, surface properties, presence of impurities, presence of other ions and time t.

The paper will present the aragonite structure of calcium carbonate deposited under controlled conditions on the steel and enamelled surfaces with different roughnesses. The specimens, prepared in this manner, were exposed to ultrasonic-generated cavitation in a vessel with sonotrode excitation.

The ultrasonic cavitation is formed by periodic oscillation of sonotrade in the liquid, causing pressure fluctuations. When the longitudinal pressure waves pass through a liquid, they form compressions (areas of pressure load/high pressure) and rarefactions (areas of tensile load/low pressure). If the oscillation amplitude is sufficiently high, the pressure in the rarefaction may decrease to the vaporisation pressure. This forms the vapour phase. Real liquid also includes dissolved gases, various solid and gas inclusions in the form of bubbles in small cracks and pockets on the surface of solid particles (Mørch, 2007; Davydov and Kedrinskii, 2003). Cavitation is a process of vapour bubble growth and collapse. During the process extremely high pressure and temperature fluctuations occur which may cause the destruction of solid walls. Two high pressure peaks may be found during one cavitation cycle. One relates to the cavitation collapse and the other one corresponds to the cavitation shed off, both contributing to a distinctive stepwise erosion damage growth pattern (Dular et al., 2013; Petkovšek and Dular, 2013). Latest cavitation research provides new insights in the mechanism of cavitation erosion

which may be interesting for scale removal. It was determined (Dular et al., 2013) that larger single pits result from several impacts of shock waves on the same area, which means that they are merely special cases of pit clusters (pit clusters where pits overlap perfectly). The indicated effects generate enough energy that may cause a local mechanical destruction of solid substance in the vicinity of the collapse of cavitation cloud. Although research (Petkovšek and Dular, 2013) was performed on thin aluminium foil, analysis of the results revealed that damage only occurs at cavitation cloud collapse that the size of the cloud and it distance from the surface at collapse do not influence the extent of the damage and that an irregular or 'broken' type of cavitation cloud causes the most damage to the foil. These data confirm that intensity cavitation erosion is difficult to evaluate from images alone, while also strong pressure pulsations alone, although below the yield stress, may still cause limited damage to the surface.

The purpose of the paper is the following. We will present a model of cavitation cloud dynamics, which we will link with the cavitation erosion. For this, we will introduce a simple estimator of relative change in the texture of specimen ε, which will be obtained from images of test samples. We want to show that scale removal is dependent on intensity of cavitation and on the surface material properties.

2 Preparation of samples: deposition of scale on the specimens

We tested four different groups of surfaces. Eighteen specimens were prepared. The specimens were assembled from substrate and sheet metal plate. The substrate was same for all specimens, while sheet metal plates with scale deposits were different for all 18 specimens. The specimen substrate was made of stainless steel. Substrate stem with M10x1 thread served for fastening to the bottom of the vessel. From the upper side, the specimen had a flat surface with a diameter of 16 mm, to which a sheet metal plate of the same diameter was fixed. Fixing of the sheet metal plate to the substrate was performed using a thin layer of the two-component water-resistant glue (Araldite 2052, Huntsman Advanced Materials). The plates were made of four different materials. Three stainless sheet metal types of different composition and roughness was used (13 specimens), while one enamelled sheet metal was used (5 specimens). The material and the roughness of surface are shown in Table 1. The roughness of surface, to which the deposition of calcium carbonate was performed, was measured using a surface roughness tester Mitutoyo SJ – 301. After the deposition of scale, the roughness was not measured.

Table 1 Data on the specimens, to which the scale was deposited

Group	*Specimen*	*Material*	*Description*	*Roughness Ra* (μm)
1	1–4	2.4858	Nickel alloy with high chemical and temperature resistance	0.30
2	5–9	1.4845	Austenitic stainless steel with excellent high-temperature resistance	0.31
3	10–14	Colorobbia AMSP 1211M	Powder enameled (Colorobbia, type AMSP 1211M) metal sheet ED4	0.16
4	15–18	1.4016	Brushed ferritic stainless steel with good corrosion resistance	0.42

The deposition of scale on the metallic and enamelled surface of specimens was carried out using an in-house designed scale deposition station shown in Figure 1. The scale deposition station consisted of a water preparation tank, a pump, deposition vessel with specimen, induction cooker, drain, measuring and control unit and personal computer. The specimens were placed into the vessel for the deposition of scale (Figure 1, detail A). Using a bolted joint, they were fastened to the bottom of the vessel that consisted of two plates. The upper 10 mm thick plate was made of stainless austenitic sheet metal and served for attachment of specimens. The lower 10 mm thick plate was made of ferromagnetic sheet metal and welded to the upper plate in the middle and along the circumference. Thus, we ensured that the bottom of the vessel was heated as equally as possible under the influence of high-frequency magnetic field generated by the induction cooker.

Figure 1 Measuring station for deposition of scale with an enlarged detail of specimen (Detail A). Specimen after the scale deposition was transferred to cavitation erosion test rig (Figure 2)

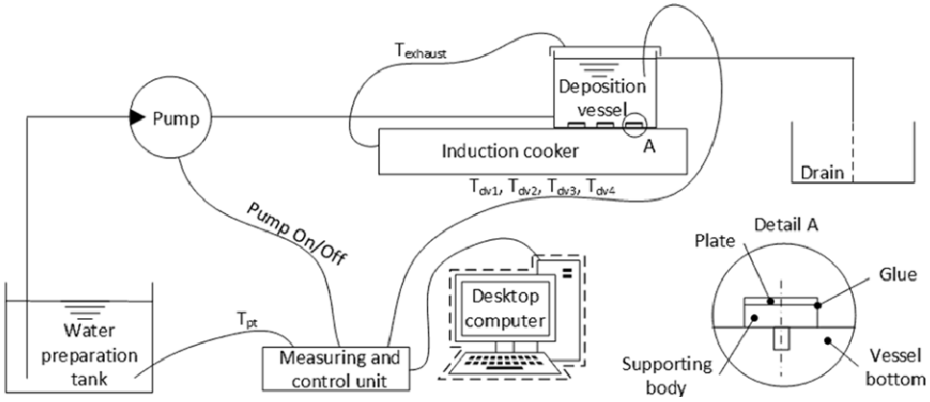

The station for the deposition of scale was composed of two subsystems. The first one regulated the operation of the flow pump, which pumped the water from the water preparation tank, in order to provide the exchange of water in the deposition vessel and capture the data on water temperature in the deposition vessel. The temperatures of water in the deposition vessel T_{dv1}, T_{dv2}, T_{dv3}, T_{dv4} were measured at four locations (three times at the height of the surface of deposition of scale to the specimens, and once just below the surface of water level in the deposition vessel). PT-100 sensors were used, located at equidistant radii from the centre of the vessel. The flow of water from the preparation vessel into the vessel for deposition of scale during the exchange was provided by the pump with a nominal water flow of 0.6 l/min, controlled by a software application in the LabView software environment.

The other system provided the appropriate temperature of water in the deposition vessel. It was based on the induction cooker Gorenje IQcook (Gorenje and Velenje, 2014), where the temperature on the exhaust T_{exhaust} of the deposition vessel was measured. For the needs of the test, we adjusted the regulation so that the temperature of water in the vessel was around 78 ± 2°C.

The water, which we used in the experiment, included high mineral content. Its hardness amounted to 19.4°dH, while its pH was practically neutral and amounted to 7.02. We manually filled the water preparation tank with water and activated both subsystems. The flow pump pumped the water into the deposition vessel above the induction cooker. During the water change, the temperature of water in the deposition vessel decreased to 30°C, but never reached the temperature of water in the water preparation tank T_{pt}, because the system started reheating the inflowing water immediately after the start of the change. In order to change all the water in the deposition vessel, the inlet of water into the vessel was placed in the wall close to the bottom of the vessel. The temperature of water in the deposition vessel reached the nominal water temperature of 78°C in the period of 25 min since the moment when the water in the deposition vessel was exchanged. In the entire period of depositing scale to the specimens, the water change mode was the same. The deposition of scale was carried out for 42 days at an increased temperature, and then the specimens waited 5 days more at an ambient temperature of ~24°C before the cavitation erosion experiment was performed. Figure 2(a) presents a typical specimen of the deposition of scale to the surface of specimen sheet metal. Figure 2(b) presents the structure of calcium carbonate at the selected segment of specimen surface.

Figure 2 Specimen 1(a) with the belonging structure (b) of scale (see online version for colours)

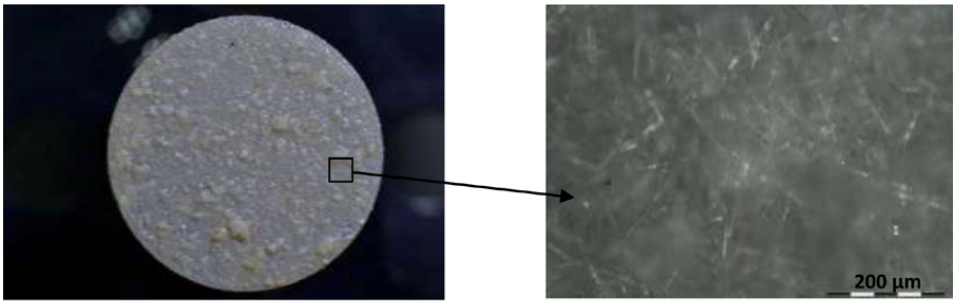

(a) (b)

The scale surface on the specimen in Figure 2(a) contains randomly distributed deposition anomalies, which are the results of the growth of crystal structure of calcium carbonate and the local anomalies on the deposition surface, which are, as a rule, related to the roughness – the geometric properties of the surface, to which the scale has been depositing. Figure 2(b) presents a micro-structure of scale surface, which, according to the shape, belongs to the aragonite structure of scale. In the structure, there is a visible basic stick structure of aragonite as the basic building block of the deposition of calcium carbonate to the metallic surface of the specimen. The average length of aragonite sticks was 80 µm.

The preparation of specimens, which is described in this chapter, was concluded with a transfer of individual specimen into the cavitation vessel, where the specimen attached itself, and we have exposed it to the ultrasonic cavitation in the subsequent phase. Before and after the cavitation, the surface of specimen was photographed as shown in Figure 2(a). The photographing conditions were identical for all the specimens in the experiment. For the photographing, we used the camera Nikon D3100 with spacers for macro photography and the lens SAMYANG AE 85 mm. The illumination was

implemented with two LED-sources, each having seven LEDs CREE XM-L U2 on an oval PCB. The illumination was located at a 10 cm distance from specimen. All LED diodes were operating at constant current of 3 A per LED diode. In comparison with complex topography measurements, this simple macro photography of specimen surface estimation provides much less data, but has proved suitable for analysis of cavitation erosion using equations (7)–(9).

3 Scale removal

The cavitation of scale specimens was performed in the ultrasonic homogeniser model CP300, series 4710, manufactured by Cole Parmer. The sonotrode was used as a source of acoustic cavitation. The experimental configuration is shown in Figure 3. The sonotrode was excited with a frequency 20 kHz and was installed coaxially to the specimen. The clearance of the sonotrode from the specimen was identical for all specimens, amounting to 7.5 mm. The diameter d of the sonotrode stem was 4.75 mm. The specimen was fastened to the bottom of a cylindrical vessel using a threaded joint. The diameter of the vessel was 150 mm. The cylindrically shaped vessel contained a constant amount of distilled water (600 ml). The temperature of water was measured before the start of each experiment and was within the range of 22 ± 1ºC. The duration of cavitation for each experiment was 4 min.

As a parameter of cavitation intensity, the electrical supply voltage for sonotrode excitation was used. We estimate that electrical supply voltage is proportional to the cavitation intensity.

For illumination, eight LEDs CREE XM-L T6 with supply current 2 A were used. The LED lights were arranged at a distance of 10 cm from the centre of specimen. In addition the illumination was provided from the background with the LED light and a lens. The lens was attached to the LED light such that the LED light was positioned in focus of the lens. In such configuration the illumination beams were almost parallel to the upper sample surface and perpendicular to the Seoul P7 LED light with a 25 mm mount lens were used. The LED light supply current was 1.6 A. The distance from the centre of specimen to the LED light was 20 cm. The detection of cavitation was performed using the visualisation of time-variable topological structures of cavitation clouds in the area between the peak of the sonotrode and the specimen, as presented in Figure 4.

Figure 3 Schematic diagram of the cavitation erosion experiment. The specimen after scale deposition from Figure 1 was mounted here in the place labelled as the specimen

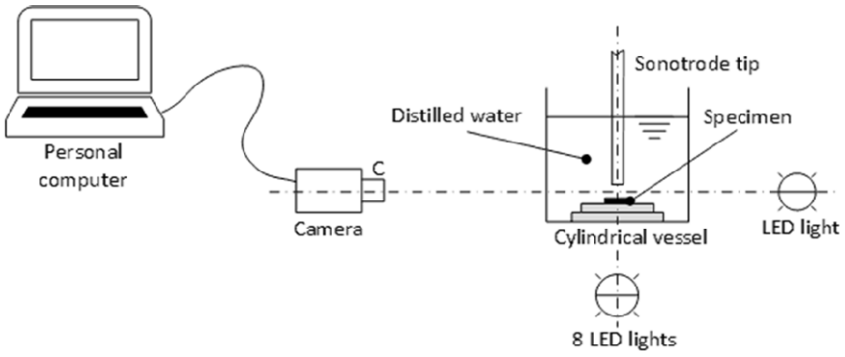

Figure 4 Time sequence of cavitation structures between the sonotrode in the upper part and the specimen in the lower part of the image $dt = 0.5$ ms

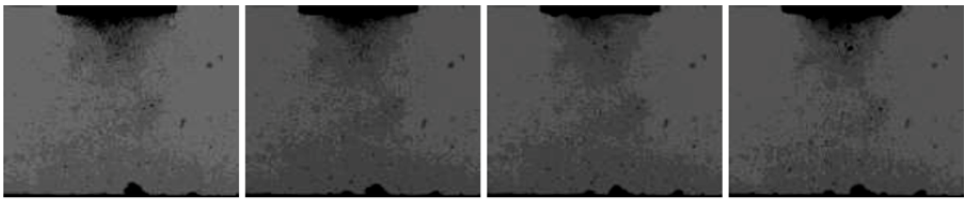

For images acquisition, the camera Hispec 4, manufactured by Fastec Imaging, was used. The camera was equipped with the lens Nikkor 50 mm 1 : 1.2. The distance of the camera sensor to the sonotrode was 33 cm. The focal point of camera lens was set to indefinite. The frequency of image capturing was 2 kHz. The number of consecutively taken images was 1000 images per each sample. The image resolution was 608 by 514 pixel. Pixel size was 15.3 μm. The size of the image was selected such that image covered entire region between the specimen and the sonotrode tip.

Quantitative analysis of surface details from Figure 4 is not possible. These figures were not intended for surface analysis, they were intended for the use with the cavitation cloud dynamics model. The surface details, as seen in Figures 4 and 5 are cavitation clouds, attached to the specimen surface. These cavitation clouds change slowly as can be seen from consecutive high speed images shown in Figure 4.

Results in Figure 4 show cavitation clouds induced by periodic oscillation of the sonotrode in the vertical direction. Cavitation appear in the form of cavitation clouds and individual cavitation bubbles between the sonotrode tip in the upper part of the image and the specimen surface in the lower part of the image. A large cavitation cloud is present at the sonotrode surface, which is shaped by an attached cavitation and the cavitation cloud which follows the kinematics of the sonotrode and decreases with distance from the sonotrode. The lower part of images in Figure 4 includes visible parts of already eroded scale as well as cavitation bubbles. For the eroded parts of scale, it is characteristic that they are can be traced in many subsequent images, which indicates that their velocity is relatively low.

Figure 5 Observation window between the tip of sonotrode and the specimen. A is estimated according to equation (3), while $\dot{A}$ in $\ddot{A}$ are time derivatives and thus calculated from $\bar{E}$ time series. For the image shown here the values are $A = 9.51 \times 10^{-4}$, $\dot{A} = 1.19$ [m], $\ddot{A} = -1.07 \times 10^{3}\,\mathrm{m^2/s}$ and $\bar{E} = 74.53$ [-]

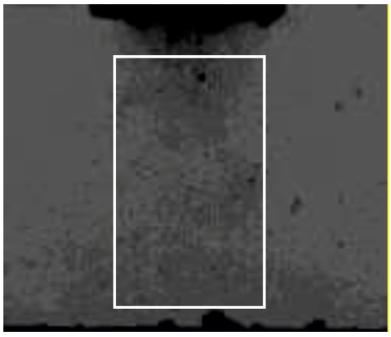

In order to connect the intensity of ultrasonic cavitation with erosion effects on the surface of specimens with the deposition of scale, the following section presents the phenomenological model of cavitation cloud dynamics. The model is able to predict the pressure waves – the pressure pulsations as a result of the dynamics of emerging cavitation clouds.

4 Model of cavitation cloud dynamics

One of the issues of cavitation erosion is the measurement of pressure fluctuations, when the specimen surface is subject to cavitation erosion. The dynamics of the spherical cavitation cloud of bubbles was already described by Brennen (1995). His model was based on the work that he had performed together with d'Agostino and Brennen (1989) and was supplemented by Shimada and Kobayashi (1990). However, measurements to confirm this cannot be performed during scale removal due to the scale debris. We have therefore used instead of pressure measurement the method of estimating pressure from the cavitation high speed imaging using the Brennen (1995) model:

$$A\left(1-\frac{\dot{A}}{c}\right)\ddot{A}+\frac{3}{2}\left(1-\frac{\dot{A}}{3c}\right)\dot{A}^2=\frac{1}{\rho_L}\left(1+\frac{\dot{A}}{c}+\frac{A}{c}\frac{\mathrm{d}}{\mathrm{d}t}\right)\left(p-p_\infty-4\frac{\mu_L}{A}\dot{A}\right) \tag{1}$$

where A [m] represents equivalent diameter of cavitation cloud of bubbles, c [m/s] speed of sound in fluid, p [N/m^2] pressure inside the cavitation cloud of bubbles, μ_L [m^2/s] fluid kinematic viscosity, ρ_L [kg/m^3] fluid density, and p_∞ [N/m^2] fluid ambient pressure. According to d'Agostino and Brennen (1989) the interface velocity $\dot{A}$ is largely subsonic with reference to the speed of sound in fluid in cloud of bubbles in water whose oscillatory dynamics is analysed in the neighbourhood of an equilibrium configuration at excitation frequencies not much larger that the natural frequency of the each individual bubble. With assumption that $c \gg \dot{A}$ the following algorithm can be used for calculation of pressure fluctuation in cavitation cloud observed:

$$A\ddot{A}+\frac{3}{2}\dot{A}^2=\frac{1}{\rho_L}\left(p-p_\infty-4\frac{\mu_L}{A}\dot{A}\right) \tag{2}$$

For the equivalent diameter of cavitation cloud A we assume proportionality to the intensity of grayscale level $\bar{E}$ [-] in observation window in Figure 5: $A \propto \bar{E}$. Similar assumptions were already reported in Bizjan et al. (2014). Under such assumption changes of cavitation cloud equivalent diameter in time t can be calculated using equation (3).

$$\bar{E}(t)=\sum_{i=1}^{i=N}\sum_{j=1}^{M}E(i,j,t);\ \ E(i,j,t)\epsilon\{1\div256\}. \tag{3}$$

In relation to equation (3), pressure fluctuations were monitored in rectangular observation window which has a size of $N \times M = 240 \times 410$ pixels. Window location is shown in Figure 5. The results of pressure fluctuation are written in time series. The pressure fluctuations are calculated from cavitation structures changes observed in selected window.

If boundary conditions and material properties of the liquid are known, then the instantaneous value of pressure $p(t)$ may be calculated from equation (2). We have used the statistical estimator π (equation (4)) as a parameter of cavitation intensity for the analysis of pressure fluctuations caused by sonotrode ultrasonic excitation.

$$\pi = \frac{\sigma_j}{\sigma_{\max,j}}, \tag{4}$$

where σ_j is the standard deviation of the selected pressure time series $p(t)$ for the specimen j, which belongs to the individual experiment on the selected specimen. $\sigma_{\max,j}$ is the maximum standard deviation among all the conducted experiments. Equation (4) sets the intensity level of pressure fluctuations $p(t)$, which is used as an integral parameter of cavitation in the assessment of erosion damage on the specimens of scale.

With the above procedure we have provided an estimation of integral pressure fluctuations above the specimen surface. In the following, we will show how parameter π is related to the cavitation erosion.

5 Evaluation of erosion effects

The intensity of cavitation erosion on the specimens, which were exposed to ultrasonic cavitation, was assessed on the basis of the change in the specimen surface. In this case, the visualisation method was used. Figure 6 presents a sample specimen of deposited scale before and after the exposure to ultrasonic cavitation (specimen 5, as shown in Table 1).

Figure 6 Specimen 5 with deposited scale: (a) before cavitation and (b) after cavitation (see online version for colours)

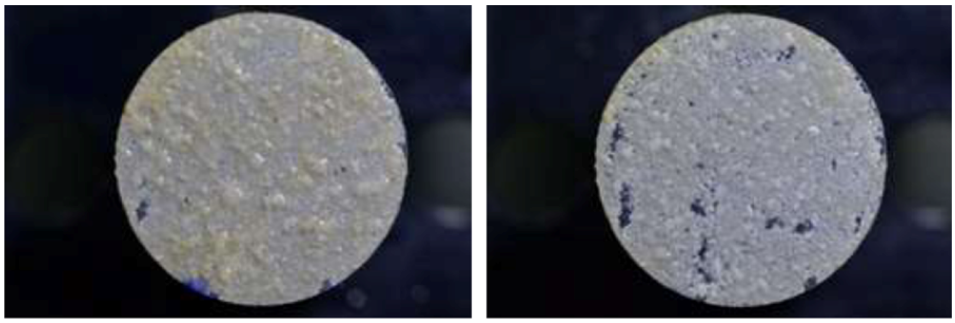

(a) (b)

Figure 6(a) presents a sample specimen after the finished deposition of scale and immediately before the performance of ultrasonic cavitation. Figure 6(b) presents the specimen scale surface after the performed cavitation. All images were recorded under identical photographing conditions as described in subsection (Scale removal). From the qualitative comparison between the textures on the photographs, we may conclude that the specimen after ultrasonic cavitation shows visible areas, where intensive erosion removed the scale up to the specimen surface. It also shows visible differences in the areas where the cavitation erosion was the cause for partial removal of scale. Partial scale

removal is expressed as the change of the scale surface. The quantitative erosion evaluation was conducted by comparing the images of specimens before and after the cavitation test. First, the specimens RGB colour images were converted into an 8-bit grey image with the pixel value of 0 for black colour and 255 for white colour. The mean value μ of grey image level intensity was assessed in the circle with radius $D/2$ in the centre of specimen. The observation area was the same in all cases. The difference of mean values before and after cavitation gives an indication of the change of specimens surface:

$$\Delta\mu = \mu_{\text{before}} - \mu_{\text{after}}. \tag{7}$$

In order to perform the comparisons between all specimens in the experiment, a relative assessment of the change of surface is submitted:

$$ER = \frac{\mu_{\text{before}} - \mu_{\text{after}}}{\mu_{\text{before}}} \tag{8}$$

which is standardised to the maximum value in the entire set of measurement.

$$\varepsilon = \frac{ER_j}{ER_{j,\max}}, \tag{9}$$

where ER_j is the calculated relative assessment of the change of surface of specimen j, while $ER_{j,\max}$ is the maximum relative change between all the specimens discussed. Relative change in the surface of specimen ε will hereinafter be used for the comparison with the standardised estimator of the standard deviations of statistical estimator π (equation (4)).

6 Results of measurement

The results of measurements of cavitation erosion are presented as the change of specimen surface before and after the cavitation. Figures 7–10 show the cavitation erosion effects on the specimens surfaces in case of the same basic specimen material (Group 1, specimens 1–4, as shown in Table 1). The specimens before cavitation are presented in figures designated with (a). Figures designated with (b) represent the specimens after the performed cavitation test. The specimens in Figures 7–10 were exposed to increasing cavitation intensities for 240 s.

Figure 7a Specimen 1 with deposited scale: (a) before cavitation and (b) after cavitation (π = 0.364(–), ε = 0.038(–))(see online version for colours)

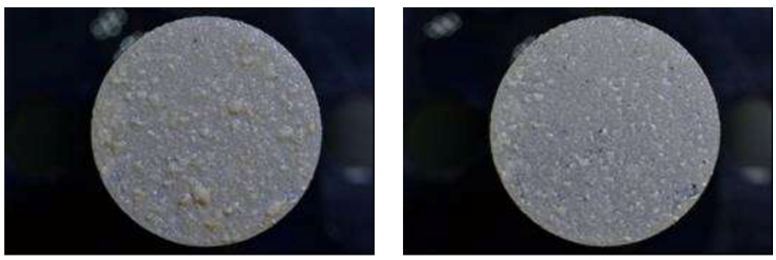

(a) (b)

Figure 7b Specimen 2 with deposited scale: (a) before cavitation and (b) after cavitation ($\pi = 0.444(–)$, $\varepsilon = 0.103(–)$) (see online version for colours)

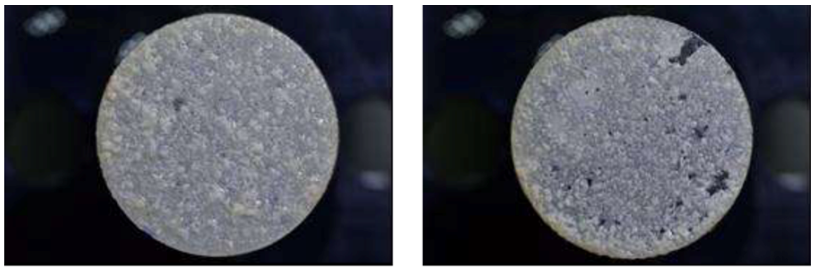

(a) (b)

Figure 7c Specimen 3 with deposited scale: (a) before cavitation and (b) after cavitation, ($\pi = 0.345(–)$, $\varepsilon = 0.141(–)$) (see online version for colours)

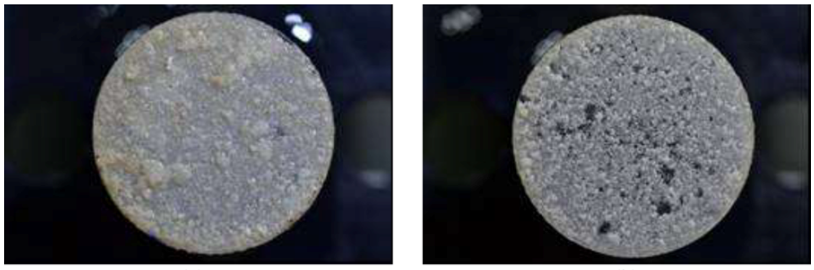

(a) (b)

Figure 7d Specimen 4 with deposited scale (a) before cavitation and (b) after cavitation ($\pi = 0.721(–)$, $\varepsilon = 0.230(–)$) (see online version for colours)

(a) (b)

Figure 8a Specimen 5 with deposited scale: (a) before cavitation and (b) after cavitation ($\pi = 0.3385(–)$, $\varepsilon = 0.046(–)$)

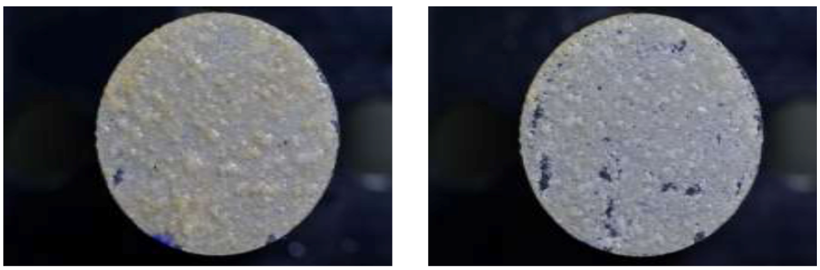

(a) (b)

Figure 8b Specimen 6 with deposited scale (a) before cavitation and (b) after cavitation (π = 0.6345(–), ε = 0.259(–)) (see online version for colours)

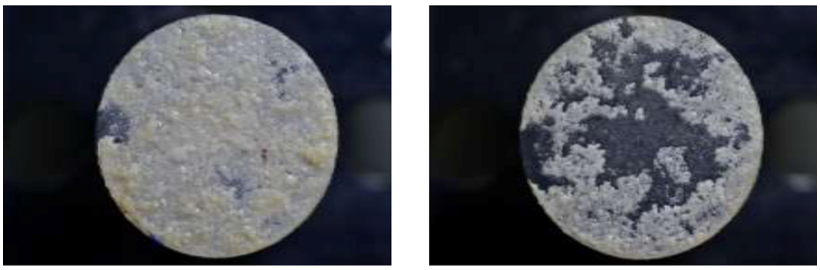

(a) (b)

Figure 8c Specimen 7 with deposited scale: (a) before cavitation and (b) after cavitation, (π = 0.547(–), ε = 0.238(–)) (see online version for colours)

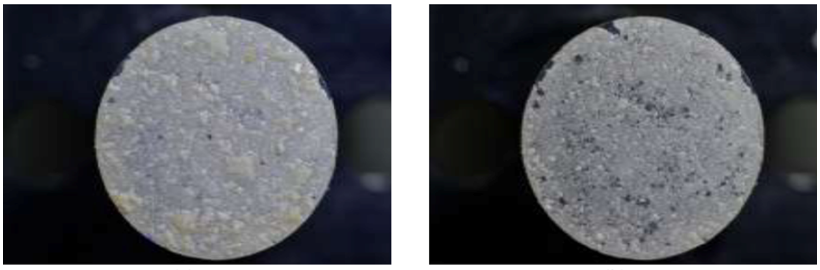

(a) (b)

Figure 8d Specimen 8 with deposited scale: (a) before cavitation and (b) after cavitation (π = 0.402(–), ε = 0.095(–)) (see online version for colours)

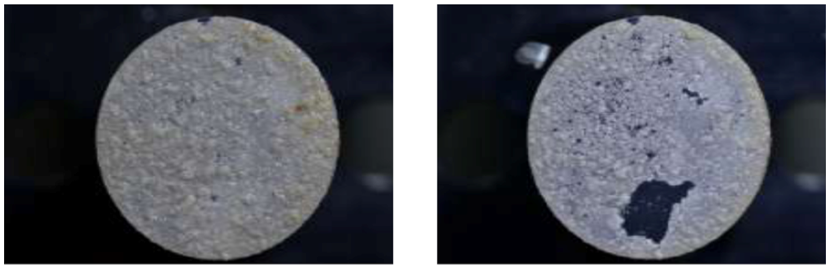

(a) (b)

Figure 8e Specimen 9 with deposited scale: (a) before cavitation and (b) after cavitation (π = 0.343(–), ε = 0.178(–)) (see online version for colours)

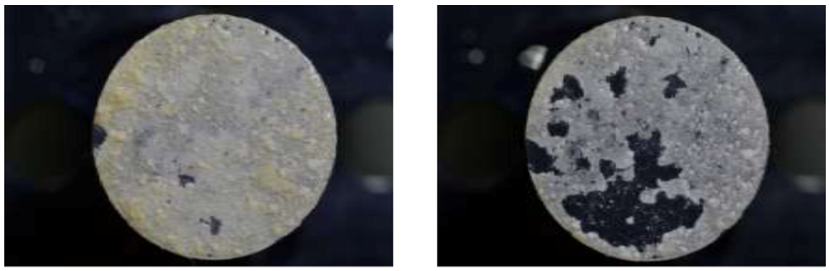

(a) (b)

Figure 9a Specimen 10 with deposited scale: (a) before cavitation and (b) after cavitation ($\pi = 0.341(–)$, $\varepsilon = 0.308(–)$) (see online version for colours)

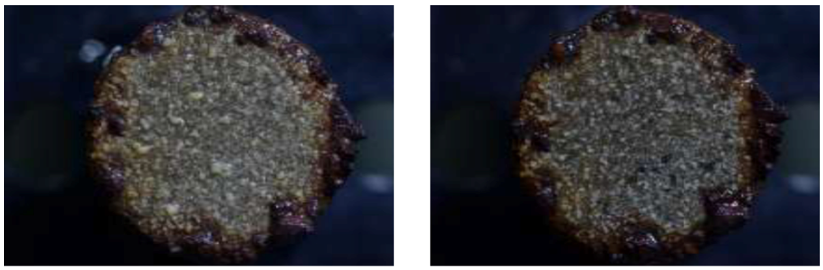

(a) (b)

Figure 9b Specimen 11 with deposited scale: (a) before cavitation and (b) after cavitation ($\pi = 0.901(–)$, $\varepsilon = 1.00(–)$) (see online version for colours)

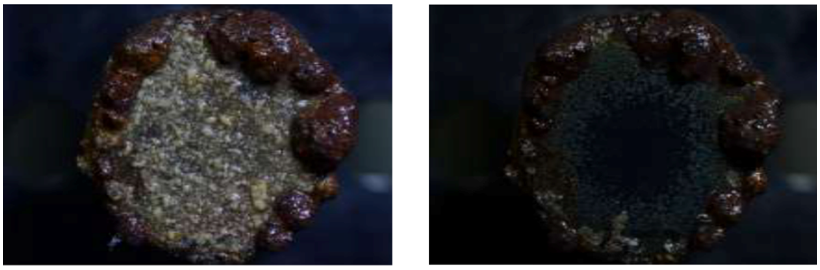

(a) (b)

Figure 9c Specimen 12 with deposited scale: (a) before cavitation and (b) after cavitation ($\pi = 0.577(–)$, $\varepsilon = 0.812(–)$) (see online version for colours)

(a) (b)

Figure 9d Specimen 13 with deposited scale: (a) before cavitation and (b) after cavitation ($\pi = 0.697(–)$, $\varepsilon = 0.793(–)$) (see online version for colours)

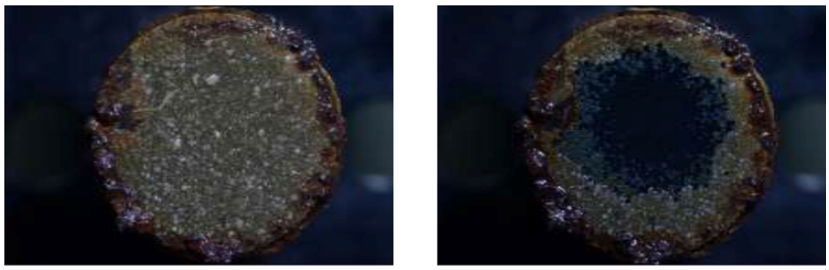

(a) (b)

Figure 9e Specimen 14 with deposited scale: (a) before cavitation and (b) after cavitation (π = 0.344(–), ε = 0.141(–)) (see online version for colours)

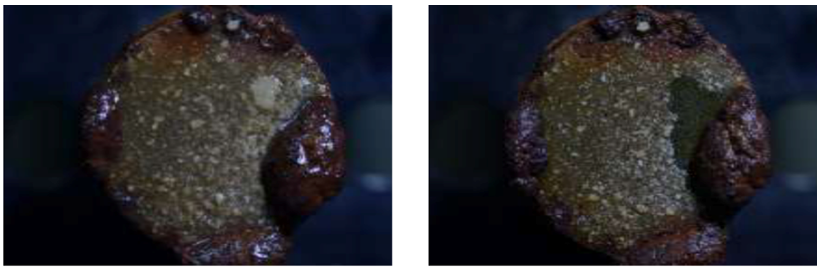

(a) (b)

Figure 10a Specimen 1 with deposited scale: (a) before cavitation and (b) after cavitation (π = 0.507(–), ε = 0.599(–)) (see online version for colours)

(a) (b)

Figure 10b Specimen 2 with deposited scale: (a) before cavitation and (b) after cavitation (π = 0.620(–), ε = 0.998(–)) (see online version for colours)

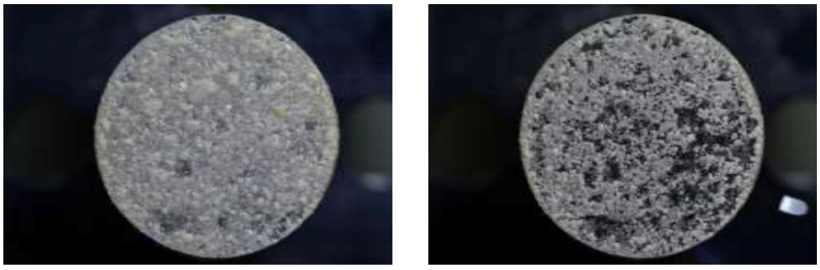

(a) (b)

Figure 10c Specimen 3 with deposited scale: (a) before cavitation and (b) after cavitation, (π = 0.335(–), ε = 0.592(–)) (see online version for colours)

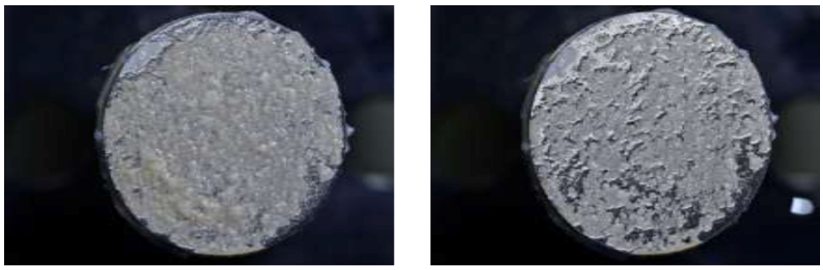

(a) (b)

Figure 10d Specimen 4 with deposited scale: (a) before cavitation and (b) after cavitation (π = 0.355(–), ε = 0.457(–)) (see online version for colours)

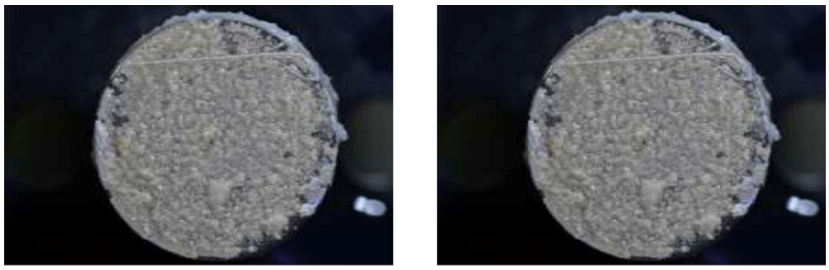

(a) (b)

The cavitation test was performed for all samples from Table 1. Results of cavitation tests are further evaluated below. In several cases, the result of cavitation test was the complete removal of scale from the specimen surface. In the case when the intensity of cavitation was low, we can notice only the changes in the scale surface, while the scale remained attached to the entire surface of the specimen (Figure 7(a)). This is mainly reflected as the modest changes of limited area and corresponding small changes in specimen surface grey level intensity. For these specimens, we did not notice the areas with complete removal of scale. The increasing intensity of cavitation increases the area of complete scale removal. In case of Figure 7(d), such an area is already very pronounced. Figure 8 shows samples from group 2, Figure 9 shows samples from group 3 and Figure 10 shows samples from Figure 10.

A quantitative analysis of erosion effects is presented in Figure 11. It is based on the implemented estimators of relative change in the surface of specimen ε (equation (9)) from the standard deviation of pressure statistical estimator π (equation (4)).

Figure 11 Model of cavitation cloud dynamics and different basic material (Ra for metal and Ra* for enamel) (see online version for colours)

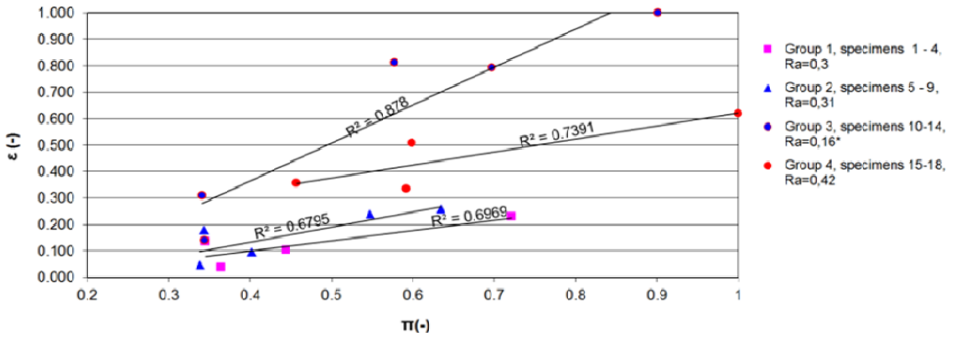

From the diagram in Figure 11, we may conclude that the intensity of pressure fluctuations affects the cavitation erosion of scale on specimens. Beside pressure fluctuations, the growth of cavitation damage mainly depends on the structure of surface and material properties of the surface, to which the scale was deposited. The most expressed damage is present on the group of specimens 3, for which a relatively small roughness of basic enamelled surface is characteristic (Ra = 0.16 μm). With regard to the

other specimens, we may notice that the difference is in both the increased erosion and the inclination angle of the regression line. In case of enamelled surface, the erosion of scale on the surface is increasing faster than in case of specimens made of steel alloys. In the group of specimens, which were made of steel alloys, we may see that the inclination angles of regression lines are approximately the same. The lowest cavitation erosion is present on the specimens of group 1 and 2, which belong to the nickel alloy with high chemical and temperature resistance and austenitic stainless steel with excellent high-temperature resistance. For both cases, we may establish that the intensity of cavitation erosion is the lowest, or that the bond between the scale and the basic surface of specimens is the strongest. The influence of material structure for the indicated groups of specimens 1 and 2 is not characteristic. Contrary to this, the intensity of cavitation erosion in the group of specimens 4 is exceeding the erosion effects on the group of specimens 1 and 2 in spite of increased level of roughness.

In brittle materials, micro-fractures appear at the onset and cracks rapidly propagate without increasing the overall applied stress. The erosion curve can still show the four characteristic stages (Thiruvengadam, 1963) of cavitation erosion since the incubation period reflects the accumulation of microcracks up to a point where material will break free. Due to the experimental procedure used here, we unfortunately cannot confirm this. Also, there are no to us known reports of cavitation erosion of scale, deposited on a substrate, with regards to the substrate surface properties.

In samples in group 2 (Ra = 0.31) in Figure 8, we see a strong tendency for spallation. We make this claim on the fact that cavitation damage in Figure 8 exhibits the sharp edges. We must compare present results with studies on surface treatments and coatings as strategies for improving cavitation erosion resistance, among them are studies investigating hard brittle coatings made of ceramics. Among them, reports (Krella, 2011) indicate failure mechanisms which include debonding, delamination and spallation. Samples in group 3 show strong tendency for delamination. Results of cavitation erosion from group 1 (Figure 7) with Ra = 0.3 or group 3 (Figure 9) does not show such properties, although group 3 exhibits the strongest dependency of cavitation erosion on pressure fluctuations as seen from Figure 11.

Additional factors contributing to scale removal include residual stresses, substrate properties and substrate coating adherence issues, porosity and interfacial defects and other imperfections (Mishnaevsky and Gross, 2004). From this, we conclude that roughness of specimen surfaces alone is unable to determine the tendency of scale layer to spallation or delamination on these specimen surfaces.

7 Conclusions

The paper presents the research of erosion effects caused by ultrasonic cavitation on metallic specimens covered by calcium carbonate – scale. The methodology of scale deposition was the same for all specimens. The ultrasonic cavitation with intensity control was selected as the generator of cavitation scale erosion. The results of experiment indicate a characteristic effect of cavitation intensity on the destruction of scale on the surface of specimens. It was established that the increasing of pressure pulsations also increases the intensity of cavitation erosion of scale on the surface of specimens as well as erosion is dependent upon the roughness of specimen surfaces,

on which the scale was deposited. The most expressed scale erosion was found on surface with smallest roughness of Ra = 0.16 μm. We have found that spallation mechanism or delamination mechanism of scale removal are not dependent solely on the roughness of specimen surfaces.

References

Bizjan, B., Orbanić, A., Širok, B., Kovač, B., Bajcar, T. and Kavkler, I. (2014) 'A computer-aided visualization method for flow analysis', *Flow Measurement and Instrumentation*, Vol. 38, August, pp.1–8.

Brennen, C.E. (1995) *Cavitation and Bubble Dynamics*, Oxford University Press, Oxford, New York.

d'Agostino, L. and Brennen, C.E. (1989) 'Linearized dynamics of spherical bubble clouds', *J. Fluid Mech.*, Vol. 199, pp.155–176.

Davydov, M.N. and Kedrinskii, V.K. (2003) 'Mathematical simulation of bubbly cluster and spall formation in a liquid at dynamic loading', *5th International Symposium on Cavitation*, Osaka, Paper No. CAV-03-GS-4-003.

DOE (2011) *Energy Savers: Tips on Saving Money and Energy at Home*, US Department of Energy, Office of Energy Efficiency and Renewable Energy, pp.1–44.

Dular, M., Coutier-Delgosha, O. and Petkovšek, M. (2013) 'Observations of cavitation erosion pit formation', *Ultrasonics Sonochemistry*, Vol. 20, No. 4, pp.1113–1120.

Elfil, H. and Roques, H. (2001) 'Role of hydrate phases of calcium carbonate on the scaling phenomenon', *Desalination*, Vol. 137, Nos. 1–3, pp.177–186.

Gorenje, D.D. and Velenje, S. (2014) *IQcook*, www.gorenje.com/iqcook/ww/ (Accessed 19 October, 2014).

Hasson, D., Shemer, H. and Sher, A. (2011) 'State of the art of friendly 'green' scale control inhibitors: a review article', *Industrial and Engineering Chemistry Research*, Vol. 50, No. 12, pp.7601–7607.

Karabelas, A.J. (2002) 'Scale formation in tubular heat exchangers – research priorities', *International Journal of Thermal Sciences*, Vol. 41, No. 7, pp.682–692.

Krella, A. (2011) 'An experimental parameter of cavitation erosion resistance for TiN coatings', *Wear*, Vol. 270, Nos. 3–4, pp.252–257.

MacAdam, J. and Parsons, S.A. (2004) 'Calcium carbonate scale formation and control', *Reviews in Environmental Science and Biotechnology*, Vol. 3, No. 2, pp.159–169.

Mishnaevsky, L.L. and Gross, D. (2004) 'Micromechanisms and mechanics of damage and fracture in thin film/substrate systems', *International Applied Mechanics*, Vol. 40, No. 2, pp.140–155.

Mørch, K.A. (2007) 'Reflections on cavitation nuclei in water', *Physics of Fluids*, Vol. 19, No. 7, pp.1–7.

Petkovšek, M. and Dular, M. (2013) 'Simultaneous observation of cavitation structures and cavitation erosion', *Wear*, Vol. 300, Nos. 1–2, pp.55–64.

Shimada, M. and Kobayashi, T. (1990) 'Dynamics of cloud cavitation and cavitation erosion', *Proceedings of the 1999 ASME Fluids Engineering Summer Meeting 1999*, San Francisco, pp.1–6.

Thiruvengadam, A. (1963) 'A unified theory of cavitation damage', *Journal of Basic Engineering*, Vol. 85, No. 3, pp.365–373.